EUROPEAN SOUTHERN OBSERVATORY

MEMORANDUM

June 8, 2005

To: D. Silva, F. Comerón, D. Baade, P. Moller, E. Jehin, K. O'Brien, A. Kaufer, M. Van Den Ancker, M. Petr, R. Mignani, G. Rupprecht, W. Freudling

From: F. Patat & M. Romaniello

Subject: Shutter Delay map for FORS1

SUMMARY

In this report we present and discuss the results of two tests which have been run to study the behaviour of FORS1 shutter. The analysis shows that the shutter error is always within specifications, i.e. less than 10 ms. Frame-to-frame random fluctuations with an RMS of 1 ms are seen, while in about 10% of the analyzed cases these reach 10 ms. Exposure times appear to be on average $\sim$5 ms shorter than the nominal value and the effective exposure time reported in the FITS header is not accurate to the level shown by observed fluctuations. If illumination gradients due to different shutter opening/closing velocity profiles are present, they must be smaller than 2 ms across the whole detector. The patterns seen in the derived delay maps are dominated by a non linearity effect, which is of the order of 0.4% at 4×10^4 ADU.

1 Introduction

Shutter-timing errors, which we will indicate here as δ, arise from the finite opening and closing time of electromechanical shutters. The δ function, which in general depends on the spatial position across the field of view, is defined in such a way that, if t is the requested integration time, the actual integration time will be $t + \delta$.
The standard procedure to derive a spatial map of $\delta(x, y)$ is based on the following considerations. If f_i $(i = 1, 2, ..., N)$ are N flat fields taken with the same exposure time t and F is a flat obtained using a single exposure time equal to Nt, one can form the ratio $r(x, y)$ between $S = \sum_{i=1}^{N} f_i$ and F. Since F is affected by only one shutter opening/closing cycle while S contains the effect of N cycles, the ratio $r = S/F$ can also be expressed as:

$$r(x, y) = \frac{N(t + \delta(x, y))}{Nt + \delta(x, y)} \tag{1}$$

which can be easily solved for $\delta(x, y)$:

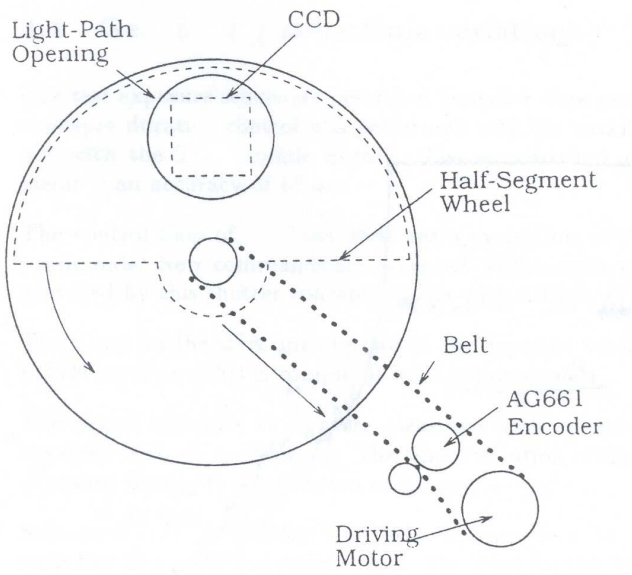

Figure 1: Schematic drawing of the FORS1 shutter (from FORS1 Final Design Report).

$$\delta(x,y) = \frac{r(x,y)-1}{N-r(x,y)}\,Nt \tag{2}$$

Of course, this procedure assumes that the flat field illumination is constant, i.e. that the flat field pattern does not change, both in shape and overall intensity, from one exposure to the next. Clearly, before forming the ratio r, all flats need to be bias subtracted, while all flat field defects in the CCD will be implicitly removed when the ratio r is computed.

2 FORS1 Shutter

The FORS1 shutter consists of a rotating half-segment wheel mounted on a light-tight metal cover and it allows a fast opening and closing of the light path in front of the CCD dewar entrance window (see Fig. 1). The wheel always moves in the same direction providing, in principle, constant exposure times for any position in the light path opening. The shutter was built according to the requirement that the time accuracy should be better than 0.01 s. In order to fulfill this specification, the shutter operates in two different ways, according to the exposure time. If this is shorter than 0.7 s, the shutter keeps moving during the exposure, with a velocity profile that was designed in order to ensure a constant spatial illumination. For exposure times longer than 0.7 s, the shutter opens, stops and finally closes. According to the FORS1 Final Design Report - Exposure Shutter Tests[1], the shutter was tested running a series of 1 s exposures, in order to check the exposure time stability. This was found to vary not more than 19 ms from frame to frame.

[1]VLT-TRE-VIC-13110-0025

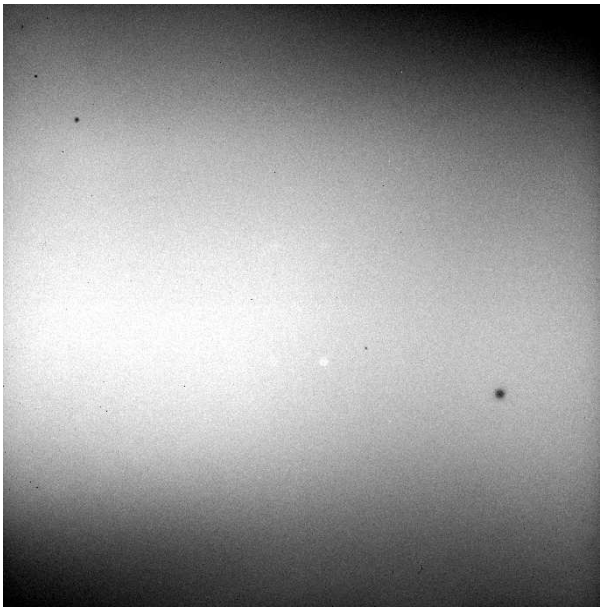

Figure 2: An example of a screen flat. The color scale is linear and ranges from 1700 (black) to 2850 (white). For presentation, the 4-port pattern was removed dividing each port by its nominal gain.

3 First test on FORS1 data

In order to characterize the shutter delay in FORS1, a first set of data was obtained on 2000-05-11. Ten screen flats, 1 s exposure each, were followed by a 10 s exposure, using the high gain and 4 port read-out mode. The frames were reduced in IRAF, applying the pre-scan correction and subtracting a master bias. An example image is shown in Fig. 2 where, for clarity, we have removed the 4-port pattern.
To give an idea of the exposure levels reached in these frames, Table 1 reports the measurements done in a 101×101 px box placed in port A and close to the center of the detector. The box size was chosen to be large enough to include a high number of px (10201) and small enough not to be affected by the large scale structure shown by the flats.
Given the typical exposure level (2800 ADU) and the gain of port A (1.46 e^-/ADU), the expected noise (also taking into account the read-out noise) is about 43.9 ADU, which is somewhat lower than the RMS values computed on the data, which vary from 45.4 to 46.5 ADU. This small difference is due to the flat field structure.
An interesting feature can be noticed looking at the values for the 10 s exposure. On the basis of the exposure level (28031 ADU), gain value and photon statistics, one would expect a RMS noise of 138.6 ADU, which is significantly lower than what is actually measured, i.e. 192.3 ADU. This is caused by the presence of small scale structure in the flats (see next section for more details).

From a purely statistical point of view, the RMS accuracy on the average exposure levels for the 1 s flats (see Table 1) is about 0.5 ADU and, therefore, the fluctuations which are seen are indeed real, reaching a peak-to-peak value of 29 ADU, i.e. 1% of the exposure level.
These variations can be ascribed to the combination of different causes, like flat field lamp stability, shutter delay and changes in the bias level. Fluctuations in the lamp flux at the level of a few tenths of a percent are plausible and, together with variable shutter times, are the most probable cause for the observed behaviour.

Average	RMS	Median
2800	45.8	2798
2797	46.5	2795
2796	45.4	2795
2794	45.5	2793
2793	45.9	2791
2822	46.3	2821
2792	45.9	2791
2793	45.4	2791
2792	45.5	2792
2793	46.2	2790
28031	192.3	28033

Table 1: Exposure levels (ADU) in the section $[800:900, 800:900]$, including 10201 px. The last row indicates the values for the 10 s exposure.

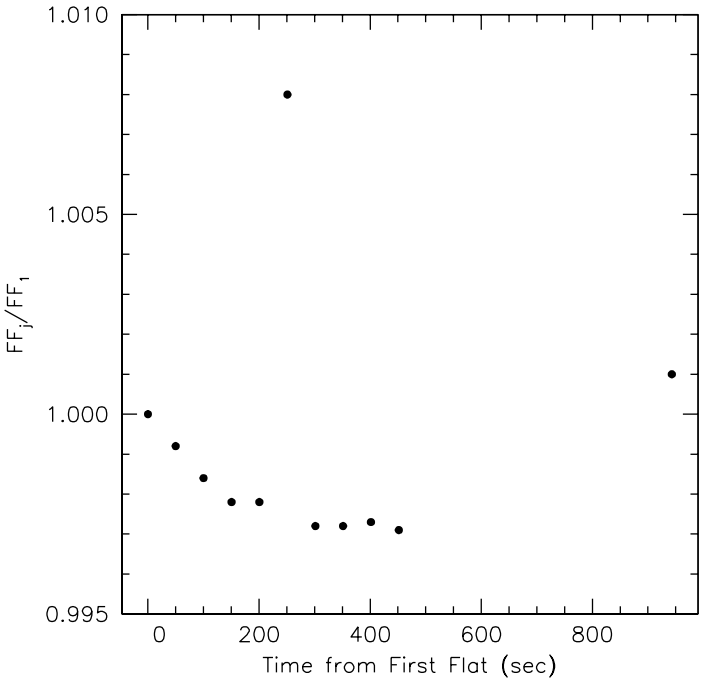

Figure 3: Flat field exposure levels normalized to the first frame as a function of starting exposure time. The last point, at about 950 s, is the exposure level of the 10 s flat divided by 10.

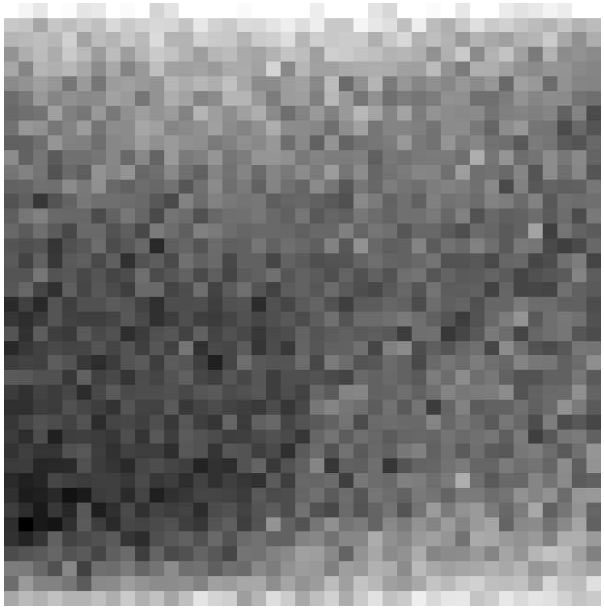

Figure 4: Shutter delay map obtained from screen flat fields. Color scale is linear between -3 (black) and $+3$ (white) ms.

In order to show how the measured flux changes with time, we have plotted in Fig. 3 the intensity of each flat after normalizing it to the first frame and then computing the average on the whole frame. Clearly this is not constant and, therefore, the assumption on which the procedure described in Sec. 1 is based, is not fulfilled.
Nevertheless, in order to run a coarse test, we have decided to multiply the first flat by 10 and use this instead of the sum of all flats. Due to the lower signal to noise one can achieve with one single flat, the final map had to be binned (50×50 px). The result is shown in Fig. 4. The variation across the whole field, if interpreted as purely due to the shutter, is about 6 ms peak-to-peak. As we will see in the next section, the observed pattern is actually not due to the shutter, but is rather related to a secondary effect which depends on the illumination level. In fact, one can immediately notice that the delay map bears a strong resemblance with the flat field illumination pattern (compare Figs. 4 and 2). More detail are given in Sec. 5.

When this data set was first analyzed in 2000, the conservative conclusion was that the peak-to-peak shutter delay is less than 10 ms, i.e. within specifications.

4 Second test on FORS1 data

Due to the renovated interest in the photometric accuracy of FORS1, we have run a second test. Given the previous experience with the exposure level fluctuations, we have chosen to use a β-light as light source rather than the screen flats. The β-light is normally used by the detector team for the linearity tests, given its extreme stability. This device is basically a glass tube filled with Tritium, which is slightly radioactive. This isotope decays emitting energy in the form of high-energy electrons (or β-rays), with a half life time of 12.3 years. The electrons then hit a phosphor compound which coats the inside of the glass Tritium tubes and this causes optical light emission.
In the case of FORS1, the β-light is mounted on one of the narrow band wheels, i.e. very close to the CCD window, hence producing a non uniform illumination, as one can see in Fig. 5,

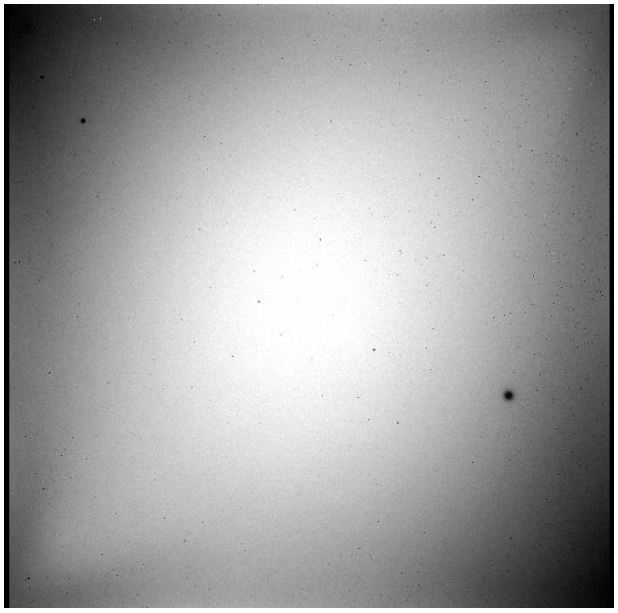

Figure 5: An example of a flat taken with the β-light. The color scale is linear and ranges from 1700 (black) to 4400 (white).

where we show an example of a flat taken with this light source.
The data were obtained on 2004-12-29 by N. Haddad, who took 10 frames with 1 s nominal exposure time each and one 10 s exposure. Just before and just after the sequence, 5 bias frames were also obtained. In order to avoid problems with the 4 port pattern removal, we have chosen to use a single port read-out, high gain (1.40 e^-/ADU).
As in the case of screen flats, we have computed the average levels of each frame in a 51×51 px box, centered on the geometrical center of the CCD. Due to the pronounced structure shown by the illumination pattern, the box size is smaller than in the previous case, but the number of pixels (2601) is still sufficient to ensure the required accuracy. The average levels and RMS deviation are reported in Table 2, together with the effective exposure times and shutter opening (t_o) and closing (t_c) times, according to the values contained in the FITS header of each image.
Already a quick look to the average values shows that, despite the usage of an extremely stable source, peak-to-peak variations of the order of 1% are still visible.
This is better illustrated in Fig. 6, where we have plotted the measured exposure levels normalized to the first frame (filled circles). While most of them are distributed close to the 1.0 nominal value, the second measurement is about 1% higher. Looking at Table 2, one can notice that in this case the effective exposure time reported by the image header is the highest of the series, suggesting that the exposure was indeed longer than the others. In order to check this suspicion, we have normalized each exposure level to the effective exposure time and overplotted the result in the same figure (empty circles).
We must notice that even though this operation brings the most deviant point closer to the others, the overall scatter does not decrease, probably indicating that the effective exposure times indicated in the headers do not reflect precisely the real values, at least not with the accuracy required here. Nevertheless, the deviations from the nominal value are within specifications (i.e. $\leq$0.01 sec) and, therefore, the shutter seems to perform as expected. The average effective exposure time is 1.0002 sec, with a RMS deviation of 0.0053 sec. Excluding the most deviant point, these values become 0.9986 sec and 0.0013 sec respectively. This

t	Average	RMS	t_o	t_c
0.9973	4202	55.9	0.193	0.191
1.0149	4245	57.2	0.188	0.197
1.0005	4203	57.3	0.192	0.186
0.9970	4200	55.5	0.196	0.190
0.9975	4193	57.4	0.194	0.193
0.9999	4204	55.5	0.197	0.196
0.9983	4205	56.4	0.197	0.198
0.9998	4202	55.7	0.198	0.196
0.9993	4200	55.6	0.191	0.185
0.9974	4202	57.1	0.194	0.193
10.0000	42221	221.4	0.190	0.189

Table 2: Relevant data for the β-light flats.

may be an indication that the distribution is not Gaussian and that, from time to time, some outlier values do occur. A more meaningful conclusion on this can be drawn only with a larger data sample.

What is interesting to note for our purpose is that the exposure level of the 10 s exposure, divided by 10 and normalized to the level of the first flat is about 0.5% higher than the average value of single 1 s flats. This already implies that in the center of the CCD, where the levels were estimated, the time delay is about -5 ms.

The map, calculated using Eq. 2 after replacing the second flat (i.e. the most deviant) with a copy of the third one, is shown in Fig. 7. As one can immediately notice, the pattern is reminiscent of the one shown by the single flats (see Fig. 5), as it was the case for the map derived from the screen flats (see Sec. 3). In this respect, we must notice that while this pattern is present in each ratio f_i/F, this is not the case for f_i/f_j (with $i \neq j$). This seems to imply that in the long exposure some additional effect related to the exposure level must be present, even though at a very low level. In fact, the ratio $r = S/F$ ranges from 0.995 to 0.997, i.e. with a peak-to-peak relative variation of about 0.2%. This is discussed in more detail in the next section.

We finally notice that while the noise measured on the 1 s exposures is in agreement with Poissonian statistics, this does not happen for the 10 s exposure, as we already noticed for the screen flats (see Sec. 3). In fact, the expected noise is 173.7 ADU, while we measure an RMS deviation of 221.4 ADU, i.e. about 50 ADU higher (see Table 2). Taken as face value, this implies the existence of an additional noise source with an RMS deviation of 137.3 ADU. This is fairly consistent with the presence of small scale structures in the flat, whose effect grows linearly with the exposure level. In fact, for a frame 10 times less exposed, this produces a RMS fluctuation of 13.7 ADU, which would turn into an excess of about 1.7 ADU with respect to the Poissonian expectation (54.8 ADU). This is in very good agreement with the average noise measured on 1 s flats (56.3 ADU), which is 1.5 ADU larger than expected.

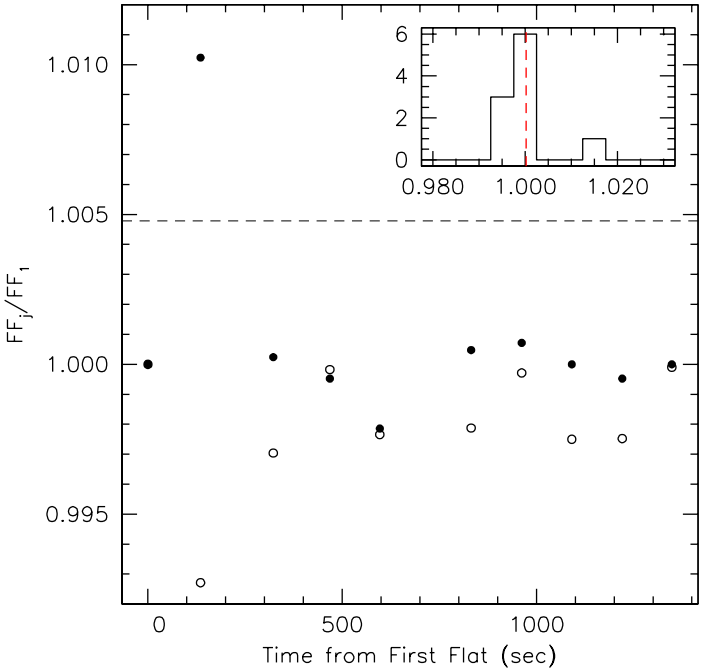

Figure 6: Normalized exposure levels for each 1 s exposure before (filled circles) and after (empty circles) the correction for effective exposure time. The horizontal dashed line is placed at the normalized exposure level for the 10 s exposure, divided by 10. The upper right panel shows the histogram of effective exposure times. The average exposure time is marked by the vertical dashed line.

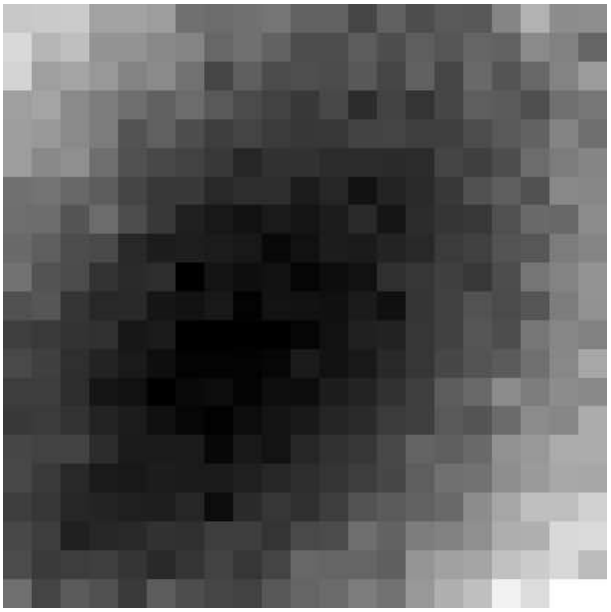

Figure 7: Shutter delay map. Color scale is linear between -5.7 ms (black) and -3.0 ms (white). To increase the signal-to-noise the original image was binned 50×50.

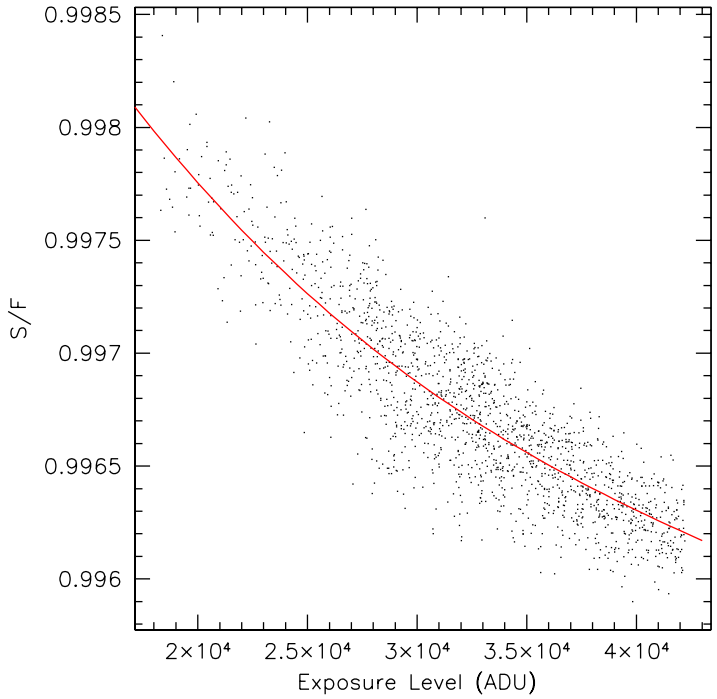

Figure 8: Intensity ratio between S and F for the β-light flats as a function of exposure level. Each point is the average ratio computed in 50×50 px bins. The solid curve is 3rd order polynomial fit.

5 Intensity Effect and numerical simulations

As we have seen in Secs. 3 and 4, there seems to be an additional effect, which must be related to the input intensity. In fact, in both data sets, the $r = S/F$ ratio shows a pattern which closely resembles that of the illumination pattern. In the absence of any additional effect, the r ratio should reflect only the shutter delay pattern, which must be totally independent from the illumination pattern. Since both in the screen flats and in the β-light images strong illumination gradients are present, this offers us the opportunity of studying this effect in some detail. For this purpose we have chosen to use the latter data set, which shows an exposure level variation of more than 60% from the center to the edges of the detector (see for example Fig. 5).

After constructing the S/F ratio and binning it 50×50 px to enhance the signal-to-noise ratio, we have plotted its value against the corresponding exposure level I of the F frame for each bin. The result is presented in Fig. 8, which shows a very clear correlation between r and I, that we have fitted with a 3rd order polynomial (solid curve):

$$r = 1.001 - 2.40 \times 10^{-7}\, I + 4.11 \times 10^{-12}\, I^2 - 2.82 \times 10^{-17}\, I^3 \qquad (3)$$

This implies that, for example, at $4{\times}10^4$ ADU the ratio is 0.2% lower than at $2{\times}10^4$ ADU or, in other words, that one measures 0.2% more photons at higher exposure levels than at lower exposure levels. Curiously enough, this effect is opposite to what one would expect from detector linearity deviations. It must be noticed that FORS1 CCD is known to have peak-to-peak linearity deviations of the order of ±0.2% in the range 0-$6{\times}10^4$ ADU, which is

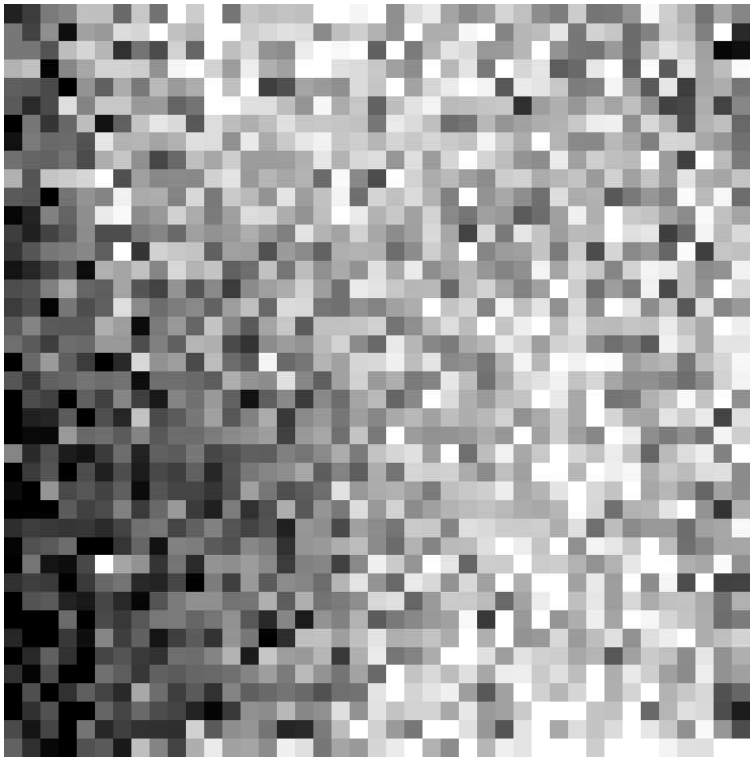

Figure 9: Shutter delay map obtained from the β-light flats after correcting for the intensity effect. The color scale is linear and ranges from $-0.2\ ms$ to $0.5\ ms$.

still compatible with the effect we see in our data[2].
If we now assume that the intensity dependency is not related to the shutter delay (which is probably not completely true, see below), we can correct r dividing it by Eq. 3 and then recompute $\delta(x, y)$ according to Eq. 2. The result of this operation is shown in Fig. 9, from which one would conclude that the peak-to-peak shutter delay is about 0.7 ms across the whole detector, with a possible gradient from the lower left corner to the upper right one.
In order to test this conclusion, we have run a numerical simulation using the following strategy. The shutter was modeled as a straight blade rotating around a given point $C(x_c, y_c)$ in the detector's coordinate system. To mimic a delay, we have introduced a constant difference in opening and closing velocities, which turns into a peak-to-peak delay variation of 5 ms. The geometry of the mechanical system was chosen to be similar to that of Fig. 1, i.e. with the rotation center in x_c=1024, y_c=−2048, which produces the shutter delay pattern shown in Fig. 10. Obviously, the iso-delay contours are straight lines pointing to the rotation center, irrespective of the velocity profile and the position of the rotation center with respect to the CCD.
The β-light illumination pattern has been reproduced using a 6th order 2D polynomial fit to the 10 s flat, which was then normalized to 1 s. Finally, the shutter delay map described above has been applied and a random noise, including photon shot noise and read-out noise (5 e^-), was added to the simulated frames. In this way, a data set including 10 exposures of 1 s and one exposure of 10 s was created and processed exactly in the same way as the real data in order to derive $\delta(x, y)$.
The simulation shows that the input shutter delay map is very well reconstructed and, therefore,

[2]See `http://www.eso.org/projects/odt/Fors1/linear.html`

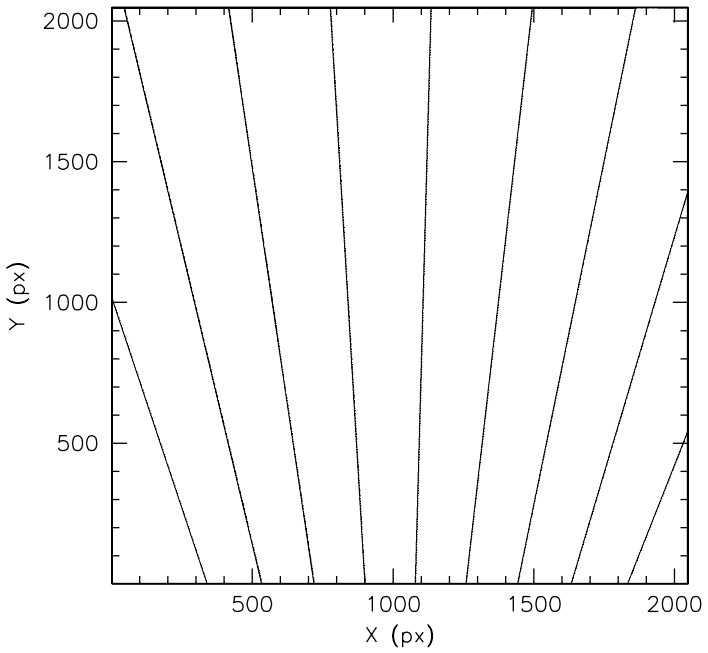

Figure 10: Simulated shutter delay contour plot. Contours are plotted every 0.5 ms, increasing from right to left.

if something similar were present in the real data, we would have clearly detected it. Moreover, given the shutter geometry which, if any, creates a monotonically increasing gradient, it is very unlikely that shutter delay effects can be confused with intensity effects. This is clearly illustrated in Fig. 11, where we have plotted r against the intensity, as we did for the real data (see Fig. 8).
Other simulations run with different positions of C show that the pattern seen in Fig. 11 is only weakly dependent on the shutter geometry, basically because the illumination pattern is roughly centrally symmetric.

6 Conclusions and Recommendations

Since no clear pattern is seen in the shutter delay map besides the one caused by the non uniform illumination present in the ingredient frames, we conclude that the spatial dependence of the shutter time delay must be small, i.e. with peak-to-peak values smaller than 5 ms.
The effective exposure times seem to be systematically shorter than the nominal values, by $\sim$5 ms. However, frame-to-frame fluctuations up to 0.01 sec are seen, which cannot be totally corrected by using the exposure times indicated in the FITS headers of the images. Indicatively, these outlier deviations occur in 10% of the cases, while in the remaining cases the exposure times appear to fluctuate around the average value with an RMS of $\sim$1 ms.
During this analysis we have found an intensity effect, which can be generally indicated as a loss of detector linearity for increasing values of the exposure level. This feature, which reaches the level of 0.4% at 4×10^4 ADU, dominates the spatial pattern of the derived shutter delay maps. If delay patterns are present, they should be on average smaller than 2 ms across the

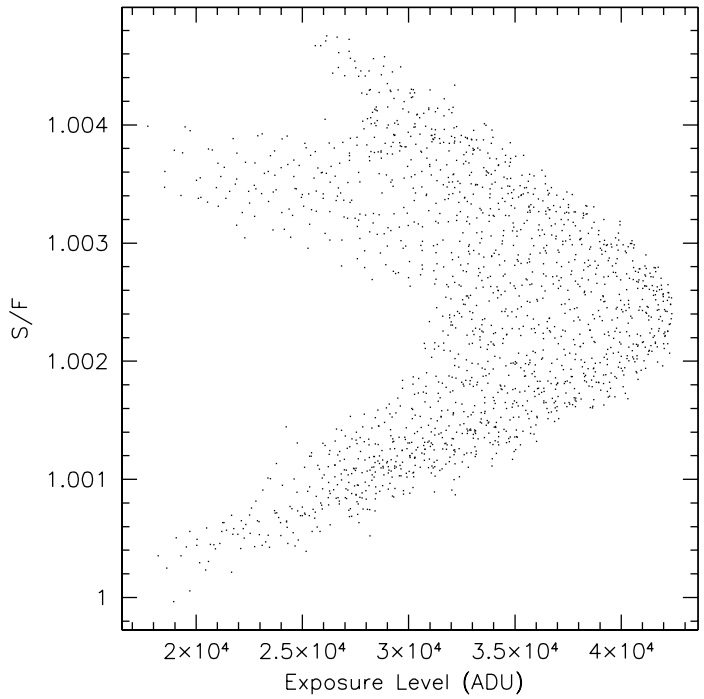

Figure 11: Intensity ratio between S and F for the simulated flats as a function of exposure level. Each point is the average ratio computed in 50×50 px bins.

whole detector.
With the currently available data, it is not possible to tell whether at this low level frame-to-frame variations are present. Also, no conclusion can be drawn about the shutter behaviour for exposure times shorter than 0.7 s, since in this regime the shutter operates in a different and the assessment of its performance requires a dedicated test.

All these findings allow us to conclude that FORS1 shutter was built within specs, i.e. with shutter time errors smaller than 10 ms. This means that in a 1 s exposure, the maximum error due to shutter inaccuracies can account up to 0.01 magnitudes, which corresponds to a photometric error of about 1%.